An Improved Bound on the Optimal Paper Moebius Band

Richard Evan Schwartz [*†]

September 16, 2023

Abstract

We show that a smooth embedded paper Moebius band must have aspect ratio at least $\phi = (1+\sqrt{5})/2 = 1.61....$ This is an improvement of the previously known bound of $\pi/2 = 1.5708....$

1 Introduction

Note: This paper has been superseded by my recent paper *The Optimal Paper Moebius Band*, (arXiv 2308.12641) which proves the Halpern-Weaver conjecture in full. Also, this paper had a mistake in it. The updated version here corrects the mistake and otherwise keeps as close as possible to the original text.

This paper addresses the following question. *What is the aspect ratio of the shortest smooth paper Moebius band?* Let's state the basic question more precisely. Given $\lambda > 0$, let

$$M_\lambda = ([0,1] \times [0,\lambda])/\sim, \qquad (x,0) \sim (1-x,\lambda) \tag{1}$$

denote the standard flat Moebius band of width 1 and height λ. This Moebius band has aspect ratio λ. Let $S \subset \boldsymbol{R}_+$ denote the set of values of λ such that

*email: Richard.Evan.Schwartz@gmail.com
†Supported by N.S.F. Grant DMS-1807320

there is a smooth [1] isometric embedding $I : M_\lambda \to \boldsymbol{R}^3$. The question above asks for the quantity

$$\lambda_0 = \inf S. \tag{2}$$

The best known result, due to Halpern and Weaver [**HW**], is that

$$\lambda_0 \in [\pi/2, \sqrt{3}]. \tag{3}$$

In §14 of their book, *Mathematical Omnibus* [**FT**], Fuchs and Tabachnikov give a beautiful exposition of the problems and these bounds. This is where I learned about the problem.

The lower bound is local in nature and does not see the difference between immersions and embeddings. Indeed, in [**FT**], a sequence of immersed examples whose aspect ratio tends to $\pi/2$ is given. The upper bound comes from an explicit construction. The left side of Figure 1.1 shows $M_{\sqrt{3}}$, together with a certain union of *bends* drawn on it. The right side shows the nearly embedded paper Moebius band one gets by folding this paper model up according to the bending lines.

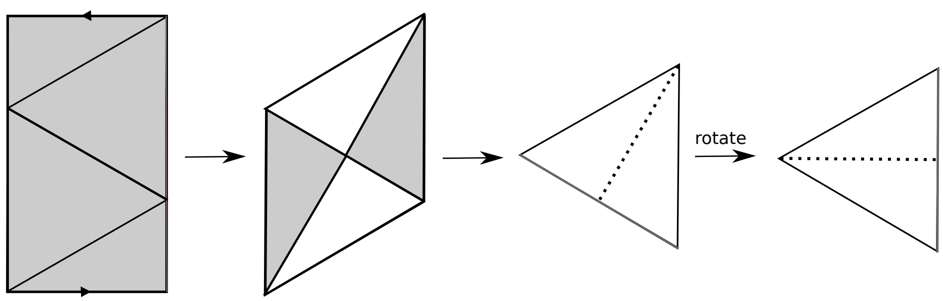

Figure 1.1: The conjectured optimal paper Moebius band

The Moebius band just described is degenerate: It coincides as a set with the equilateral triangle Δ of semi-perimeter $\sqrt{3}$. However, one can choose any $\epsilon > 0$ and find a nearby smoothly embedded image of $M_{\sqrt{3}+\epsilon}$ by a process of rounding out the folds and slightly separating the sheets. Halpern and

[1]The smoothness requirement (or some suitable variant) is necessary in order to have a nontrivial problem. Given any $\epsilon > 0$, one can start with the strip $[0, 1] \times [0, \epsilon]$ and first fold it (across vertical folds) so that it becomes, say, an $(\epsilon/100) \times \epsilon$ "accordion". One can then easily twist this "accordion" once around in space so that it makes a Moebius band. The corresponding map from M_ϵ is an isometry but it cannot be approximated by smooth isometric embeddings.

Weaver conjecture that $\lambda_0 = \sqrt{3}$, so that the triangular example is the best one can do.

The Moebius band question in a sense goes back a long time, and it is related to many topics. The early paper [**Sad**] proves rigorously that smooth paper Moebius bands exist. (See [**HF**] for a modern translation to english.) The paper [**Sab**] studies the extrinsic geometry of flat Moebius bands embedded or immersed into Euiclidean space. The paper [**SU**] establishes various structural results about flat surfaces with singularities embedded in $\boldsymbol{R}^3$. The paper [**CF**] gives a general framework for considering the differential geometry of developable surfaces.

Some authors have discussed optimal shapes for Moebius bands from other perspectives, e.g. algebraic or physical. See, e.g. [**MK**] and [**S1**]. The Moebius band question has connections to origami. See e.g. the beautiful examples of isometrically embedded flat tori [**AHLM**]. It is also related to the main optimization question from geometric knot theory: What is the shortest piece of rope one can use to tie a given knot? See e.g. [**CKS**].

In this paper we improve the lower bound. Because we do not want to worry about possible pathologies, we assume explicitly that the smooth extension of our map I to a neighborhood of M_λ is regular in the sense that the differential dI is 1-to-1 everywhere. This regularity will help us when we make polygonal approximations. We don't want to worry about any funny behavior at the boundary of M_λ.

Theorem 1.1 (Main) *An embedded paper Moebius band must have aspect ratio at least* $\phi = (1+\sqrt{5})/2$.

The proof of the Main Theorem has 2 ideas, which we now explain. Being a ruled surface, $I(M_\lambda)$ contains a continuous family of line segments which have their endpoints on $\partial I(M_\lambda)$. We call these line segments *bend images*. Say that a T-*pattern* is a pair of disjoint perpendicular coplanar bend images. The T-pattern looks somewhat like the two vertical and horizontal segments on the right side of Figure 1.1 except that the two segments are disjoint in an embedded example. Here is our first idea.

Lemma 1.2 *An embedded paper Moebius band of aspect ratio less than* $7\pi/12$ *contains a* T*-pattern.*

Note that $7\pi/12 > \sqrt{3}$, so Lemma 1.2 applies to the examples of interest to us. The immersed examples in [**FT**] do not have these T-patterns, and it is illuminating to sketch the idea of the proof of Lemma 1.2 and see where it breaks down for immersed examples. The proof does not break down until the very end.

Proof Sketch: We will consider pairs of bend images whose directions are perpendicular. Call these *perpendicular pairs*. We will use a homological argument to produce a continuous path, though perpendicular pairs, which starts at a perpendicular pair and returns to the same pair but with the two bend images switched. A perpendicular pair determines a unique pair of parallel planes, one containing each of the bend images in the pair. As we go along our path, the original pair of planes must return to itself, but with the planes switched. If the planes are to remain disjoint they must sort of turn over each other. Once we suitably rotate the Moebius band, the bound of $7\pi/12$ will keep all the bend images horizontal enough to prevent this turnover. So, what happens is that the planes coincide at some moment along the path. At this moment the bend images are perpendicular and coplanar. *Since the Moebius band is embedded*, this gives us a T-pattern. In the immersed case, these coplanar perpendicular segments could cross each other like a + sign.

The two bend images comprising the T-pattern divide $I(M)$ into two halves. Our second idea is to observe that the image $I(\partial M_\lambda)$ makes a loop which hits all the vertices of the T-pattern. The convex hull of the T-pattern contains a triangle of base at least 1 and height at least 1. Such a triangle has semi-perimeter at least the golden ratio, 1.61.... Hence λ_0 is at least the golden ratio.

In §2 we introduce polygonal paper Moebius bands and some basic geometric objects associated to them. We then prove Lemma 1.2 for polygonal Moebius bands. The smooth case follows from a routine approximation argument.

I would like to thank Dan Cristofaro-Gardiner, Dmitry Fuchs, Steve Miller, and Sergei Tabachnikov for helpful discussions about this problem. I would especially like to thank Sergei for telling me about the problem and pointing me to his book with Dmitry. I would also like to acknowledge the support of the Simons Foundation, in the form of a 2020-21 Simons Sabbatical Fellowship, and also the support of the Institute for Advanced Study, in the form of a 2020-21 membership funded by a grant from the Ambrose Monell Foundation.

2 Existence of the T Pattern

2.1 Polygonal Moebius Bands

Basic Definition: Let M_λ be the Moebius band in Equation 1. Say that a *special triangle* in M_λ is a triangle whose vertices all lie in ∂M_λ. A *special triangulation* of M_λ is a triangulation consisting entirely of special triangles. The left side of Figure 1.1 shows an example. Say that a *polygonal Moebius band* is a pair $\mathcal{M} = (\lambda, I)$ where $I : M_\lambda \to \boldsymbol{R}^3$ is a map which is an isometry on each triangle of some special triangulation of M_λ. We work entirely with polygonal Moebius bands. In the last chapter we explain why the results in the polygonal case imply the results in the smooth case.

Associated Objects: Let $\delta_1, ..., \delta_n$ be the successive triangles of the special triangulation associated to $\mathcal{M}$.

- The *ridge* of δ_i is edge of δ_i that is contained in ∂M_λ.
- The *apex* of δ_i to be the vertex of δ_i opposite the ridge.
- A *bend* is a line segment of δ_i connecting the apex to a ridge point.
- A *bend image* is the image of a bend under I.
- A *facet* is the image of some δ_i under I.

We always represent M_λ as a parallelogram with top and bottom sides identified. We do this by cutting M_λ open at a bend. See Figure 2.1 below.

The Sign Sequence: Let $\delta_1, ..., \delta_n$ be the triangles of the triangulation associated to $\mathcal{M}$, going from bottom to top in P_λ. We define $\mu_i = -1$ if δ_i has its ridge on the left edge of P_λ and $+1$ if the ridge is on the right. The sequence for the example in Figure 1.1 is $+1, -1, +1, -1$. In general, the signs need not alternate like this.

The Core Curve: There is a circle γ in M_λ which stays parallel to the boundary and exactly 1/2 units away. In Equation 1, this circle is the image of $\{1/2\} \times [0, \lambda]$ under the quotient map. We call $I(\gamma)$ the *core curve*.

The left side of Figure 2.1 shows M_λ and the pattern of bends. The vertical white segment is the bottom half of γ. The right side of Figure

2.1 (which has been magnified to show it better) shows $I(\tau)$ where τ is the shaded half of M_λ. All bend angles are π and the whole picture is planar. The grey shaded curve on the right is the corresponding half of the core curve.

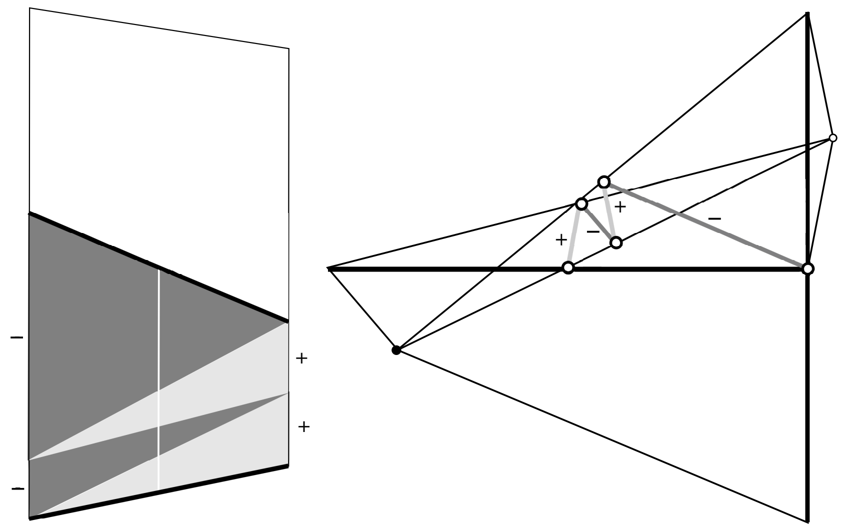

Figure 2.1: The bend pattern and the bottom half of the image

The Ridge Curve: We show the picture first, then explain.

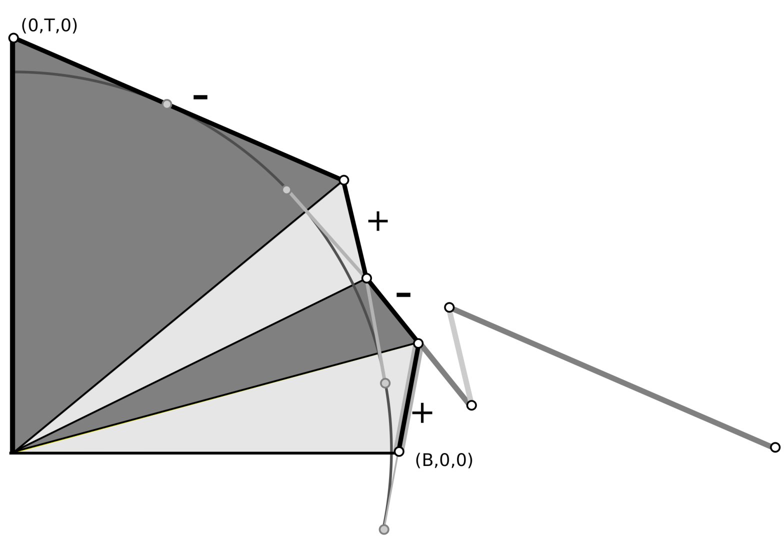

Figure 2.2: Half 2x core curve (grey) and half ridge curve (black).

Let β_b be the bottom edge of the parallelogram representing M_λ. We normalize so that I maps the left vertex of β_b to $(0,0,0)$ and the right vertex to $(B,0,0)$, where B is the length of β_b. Let $E_1,...,E_n$ be the successive edges of the core curve, treated as vectors. Let

$$\Gamma'_i = 2\mu_i E_i, \qquad i=1,...,n. \tag{4}$$

Let Γ be the curve whose initial vertex is $(B,0,0)$ and whose edges are $\Gamma'_1,...,\Gamma'_n$. Here $\mu_1,...,\mu_n$ is the sign sequence.

Let $C\Gamma$ be the cone of Γ to the origin. The cone $C\Gamma$ is triangulated by triangles $\Delta_1,...,\Delta_n$, where each Δ_i is the translate of $\mu_i I(\delta_i)$ whose apex is at the origin. In particular, the vectors pointing to the vertices of Γ are parallel to the corresponding bend images and have the same length. Figure 2.2 shows the portion of the ridge curve (in black) associated to the example in Figure 2.1. We have also scaled the core curve by 2 and translated it to show the relationships better.

Lemma 2.1 *Γ connects $(B,0,0)$ to $(-B,0,0)$, has length 2λ, and is disjoint from the open unit ball.*

Proof: By definition Γ starts at $(B,0,0)$. By construction, the segments joining the origin to the two endpoints of Γ are parallel to the same bend and have the same length. Hence Γ ends at $(\pm B,0,0)$. To rule out $(+B,0,0)$ here, we note that our process can be done on the double cover $\widetilde{M}_\lambda$ of M_λ. The map $\widetilde{I}:\widetilde{M}_\lambda \to \boldsymbol{R}^3$ is defined by composing I with the covering map. All the same constructions work. Let τ be the first triangle of M_λ and let $\widetilde{\tau}_1$ and $\widetilde{\tau}_2$ be the two triangles of $\widetilde{M}_\lambda$ covering τ. The signs associated to these two triangles are opposite. Hence, in the corresponding cone $\widetilde{C\Gamma}$, which extends $C\Gamma$, the corresponding triangles are images of each other under a point reflection. This implies that Γ ends at at $(-B,0,0)$.

There is a piecewise isometric bijection between ∂M_λ and Γ. Since ∂M_λ has length 2λ so does Γ. Say that the *lone vertex* of a special triangle of M_λ is the vertex which is the one opposite the side of the triangle that lies in ∂M_λ. The distance from the lone vertex of a special triangle to the line extending the opposite edge is 1. But this means that the distance from the origin to the line extending the corresponding edge of Γ is 1. Such lines are tangent to the unit sphere and remain outside the interior of the unit ball. Since we can say this for each of the edges of Γ, this means that Γ is disjoint from the open unit ball. ♠

2.2 Geometric Bounds

While we are in the neighborhood, we re-prove the lower bound from [**FT**]. The proof in [**FT**] is somewhat similar, though it does not use the ridge curve. Let λ be the aspect ratio of the polygonal Moebius band $\mathcal{M}$ and let Γ be the associated ridge curve. Let $f : \boldsymbol{R}^3 - B^3 \to S^2$ be orthogonal projection. The map f is arc-length decreasing. Letting $\Gamma^* = f(\Gamma)$, we have $|\Gamma^*| < |\Gamma| = 2\lambda$. Since Γ^* connects a point on S^2 to its antipode, $|\Gamma^*| \geq \pi$. Hence $\lambda > \pi/2$.

Now we use the same idea in a different way.

Lemma 2.2 *Suppose $\mathcal{M}$ has aspect ratio less than $7\pi/12$. Then the ridge curve Γ lies in the open slab bounded by the planes $Z = \pm 1/\sqrt{2}$.*

Proof: We divide Γ into halves. One half goes from $(B, 0, 0)$ to $(0, T, 0)$ and the second half goes from $(0, T, 0)$ to $(-B, 0, 0)$. Call the first half Γ_1. Suppose that Γ_1 intersects the plane $Z = 1/\sqrt{2}$. Then the spherical projection Γ_1^* goes from $A = (1, 0, 0)$ to some unit vector $B = (u, v, 1/\sqrt{2})$ to $C = (0, 1, 0)$. Here $u^2 + v^2 = 1/2$. The shortest path like this is the geodesic bigon connecting A to B to C. Such a bigon has length at least

$$\arccos(A \cdot B) + \arccos(B \cdot C) = \arccos(u) + \arccos(v) \geq^* 2\arccos(1/2) = 2\pi/3.$$

The starred inequality comes from the fact that the minimum, subject to the constraint $u^2 + v^2 = 1/2$, occurs at $u = v = 1/2$.

We have just shown that Γ_1 has length at least $2\pi/3$. But Γ_2 has length at least $\pi/2$ because it connects $(0, T, 0)$ to $(-B, 0, 0)$ and remains outside the open unit ball. This means that

$$\text{length}(\Gamma) = \text{length}(\Gamma_1) + \text{length}(\Gamma_2) \geq 2\pi/3 + \pi/2 = 7\pi/6.$$

This exceeds twice the aspect ratio of $\mathcal{M}$. This is a contradiction. The same argument works if Γ_1 hits the plane $Z = -1/\sqrt{2}$. Likewise the same argument works with the roles of Γ_1 and Γ_2 interchanged. ♠

Corollary 2.3 *Suppose $\mathcal{M}$ has aspect ratio less than $7\pi/12$. Let β_1^* and β_1^* be two perpendicular bend images. Then a plane parallel to both β_1^* and β_2^* cannot contain a vertical line.*

Proof: Every bend image is parallel to some vector from the origin to a point of Γ. By the previous result, such a vector makes an angle of less than $\pi/4$ with the XY-plane. Hence, all bend images make angles of less than $\pi/4$ with the XY-plane.

Suppose our claim is false. Then there is a plane Π parallel to two perpendicular bend images contains a vertical line. Let η be a unit normal to Π. This means that the vector $(0,0,1)$ is perpendicular to η. But then $\eta = (x,y,0)$ for some x,y. We can rotate the picture about the z-axis, without changing the hypotheses, so that $\eta = (1,0,0)$.

So now we have the following situation. There are 2 perpendicular vectors V_1 and V_2, both making an angle of less than $\pi/4$ with the XY-plane, which lie in the YZ plane. Let σ denote the slope function for vectors in the YZ-plane. We mean that $\sigma(x,y,z) = z/y$. The perpendicularity gives the well-known formula

$$\sigma(V_1)\sigma(V_2) = -1. \tag{5}$$

The angle condition gives $|\Sigma(V_j)| < 1$ for $j = 1,2$. This gives us a contradiction to Equation 5. ♠

2.3 Perpendicular Lines

As a prelude to the work in the next section, we prove a few results about lines and planes. Say that an *anchored line* in $\boldsymbol{R}^3$ is a line through the origin. Let Π_1 and Π_2 be planes through the origin in $\boldsymbol{R}^3$.

Lemma 2.4 *Suppose that* Π_1 *and* Π_2 *are not perpendicular. The set of perpendicular anchored lines* (L_1, L_2) *with* $L_j \in P_j$ *for* $j = 1,2$ *is diffeomorphic to a circle.*

Proof: For each anchored line $L_1 \in \Pi_1$ the line $L_2 = L_1^{\perp} \cap \Pi_2$ is the unique choice anchored line in Π_2 which is perpendicular to L_1. The line L_2 is a smooth function of L_1. So, the map $(L_1, L_2) \to L_1$ gives a diffeomorphism between the space of interest to us and a circle. ♠

A *sector* of the plane Π_j is a set linearly equivalent to the union of the $(++)$ and $(--)$ quadrants in $\boldsymbol{R}^2$. Let $\Sigma_j \subset \Pi_j$ be a sector. The boundary $\partial\Sigma_j$ is a union of two anchored lines.

Lemma 2.5 *Suppose (again) that the planes Π_1 and Π_2 are not perpendicular. Suppose also that no line of $\partial\Sigma_1$ is perpendicular to a line of $\partial\Sigma_2$. Then the set of perpendicular pairs of anchored lines (L_1, L_2) with $L_j \in \Sigma_j$ for $j = 1, 2$ is either empty or diffeomorphic to a closed line segment.*

Proof: Let S^1 denote the set of perpendicular pairs as in Lemma 2.4. Let $X \subset S^1$ denote the set of those pairs with $L_j \in \Sigma_j$. Let π_1 and π_2 be the two diffeomorphisms from Lemma 2.4. The set of anchored lines in Σ_j is a line segment and hence so is its inverse image $X_j \subset S^1$ under π_j. We have $X = X_1 \cap X_2$. Suppose X is nonempty. Then some $p \in X$ corresponds to a pair of lines (L_1, L_2) with at most one $L_j \in \partial\Sigma_j$. But then we can perturb p slightly, in at least one direction, so that the corresponding pair of lines remains in $\Sigma_1 \times \Sigma_2$. This shows that $X_1 \cap X_2$, if nonempty, contains more than one point. But then the only possibility, given that both X_1 and X_2 are segments, is that their intersection is also a segment. ♠

2.4 The Space of Perpendicular Pairs

We prove the results in this section more generally for piecewise affine maps $I : M_\lambda \to \boldsymbol{R}^3$ which are not necessarily local isometries. The reason for the added generality is that it is easier to make perturbations within this category. Let $\boldsymbol{X}$ be the space of such maps which also satisfy the conclusion of Corollary 2.3. (In this section we will not use this property but in the next section we will.) So, $\boldsymbol{X}$ includes all the isometric polygonal Moebius bands of aspect ratio less than $7\pi/12$ that we have been considering so far.

The notions of bend images and facets makes sense for members of $\boldsymbol{X}$. Recall that a bend image is the image under the map $I : M_\lambda \to \boldsymbol{R}^3$ of a bend. Most of these bends are not also edges of the special triangles in the triangulation of M_λ. We say that a *special bend* is a bend which is contained in the boundary of a special triangle. Each special bend is contained in the boundary of two such triangles. We say that a *special bend image* is the image of a special bend under I.

Lemma 2.6 *The space $\boldsymbol{X}$ has a dense set $\boldsymbol{Y}$ which consists of members such that no two facets lie in perpendicular planes and no two special bend images are perpendicular.*

Proof: One can start with any member of $\boldsymbol{X}$ and postcompose the whole map with a linear transformation arbitrarily close to the identity so as to get a member of $\boldsymbol{Y}$. The point is that we just need to destroy finitely many perpendicularity relations. ♠

We find it convenient to work with $\boldsymbol{Y}$ rather than $\boldsymbol{X}$. Given a member $\mathcal{M}$, of $\boldsymbol{Y}$ let $\mathcal{P}$ denote the space of pairs of bends in M_λ whose images under I are perpendicular. We can equally well think of $\mathcal{P}$ as the space of perpendicular pairs of bend images. The two views are completely equivalent.

Let γ be center circle of M_λ. We can identify the space of bends of $\mathcal{M}$ with γ: Each bend crosses γ exactly once and each point of γ is crossed by a unique bend. The space of ordered pairs of unequal bends can be identified with $\gamma \times \gamma$ minus the diagonal. We compactify this space by adding in 2 boundary components. One of the boundary components comes from approaching the main diagonal from one side and the other comes from approaching the diagonal from the other side. The resulting space A is an annulus. Thus, we consider $\mathcal{P}$ as a subset of A.

Lemma 2.7 *$\mathcal{P}$ is a piecewise smooth* 1*-manifold in A.*

Proof: We apply Lemma 2.5 to the the following objects:

- The planes through the origin parallel to the facets;
- The anchored lines parallel to the bend images within the facets. Within a single facet the bend images and the corresponding anchored lines are in smooth bijection.

By Lemma 2.5, the space $\mathcal{P}$ is the union of finitely many smooth connected arcs. Each arc corresponds to an ordered pair of facets which contains at least one point of $\mathcal{P}$. Each of these arcs has two endpoints. Each endpoint has the form (β_1^*, β_2^*) where exactly one of these bend images is special. Let us say that β_1^* is special. Then β_1^* is the edge between two consecutive facets, and hence (β_1^*, β_2^*) is the endpoint of exactly 2 of the arcs. Hence the arcs fit together to make a piecewise smooth 1-manifold. ♠

Now we come to the topological part of the proof. We say that a component of $\mathcal{P}$ is *essential* if it separates the boundary components of A.

Lemma 2.8 *$\mathcal{P}$ has an odd number of essential components.*

Proof: An essential component, being embedded, must represent a generator for the first homology $H_1(A) = \boldsymbol{Z}$. By duality, a transverse arc running from one boundary component of A to the other intersects an essential component an odd number of times and an inessential component an even number of times. Let a be such an arc. Each point of a corresponds to a pair of bends, which through the map I corresponds to a pair of bend images. As we move along a the angle between the corresponding bend images can be chosen continuously so that it starts at 0 and ends at π. Therefore, a intersects $\mathcal{P}$ an odd number of times. But this means that there must be an odd number of essential components of $\mathcal{P}$. ♠

2.5 The Main Argument

Now we prove Lemma 1.2. Let $\mathcal{M}$ be an (isometric) polygonal Moebius band of aspect ratio less than $7\pi/12$. There are members of $\boldsymbol{Y}$ arbitrarily close to $\mathcal{M}$. To show that $\mathcal{M}$ has a T-pattern it suffices to show that any member of $\boldsymbol{Y}$ sufficiently close to $\mathcal{M}$ has a T-pattern, because then we can take a limit of such T-patterns and get one for $\mathcal{M}$.

Relative to any member of $\boldsymbol{Y}$, the space $\mathcal{P}$ is a piecewise smooth 1-manifold of the annulus A with an odd number of essential components. The involution ι, given by $\iota(p_1, p_2) = (p_2, p_1)$, is a continuous involution of A which preserves $\mathcal{P}$ and permutes the essential components. Since there are an odd number of these, ι preserves some essential component of $\mathcal{P}$. But this means we can find a continuous path $\mathcal{K}$ in $\mathcal{P}$ which joins a pair (β_1^*, β_2^*) of perpendicular bend images to the switched pair (β_2^*, β_1^*).

Each element of $\mathcal{K}$ determines a unique pair of parallel planes, one containing each bend. If we choose our member of $\boldsymbol{Y}$ sufficiently close to $\mathcal{M}$, then by compactness and Corollary 2.3 none of the planes we encounter while moving along $\mathcal{K}$ contains a vertical line. Hence, our planes intersect the Z-axis in single and continuously varying points. As we move along $\mathcal{K}$, these Z-intercepts change places and hence at some moment coincide. At this moment, the two parallel planes are the same plane. The corresponding bends make a T-pattern.

This completes the proof.

3 References

[**AHLM**] A. Malaga, S. Lèlievre, E. Harriss, P. Arnoux,
ICERM website: https://im.icerm.brown.edu/portfolio/paper-flat-tori/ (2019)

[**CF**] Y. Chen and E. Fried, *Mobius bands, unstretchable material sheets and developable surfaces*, Proceedings of the Royal Society A, (2016)

[**CKS**] J. Cantarella, R. Kusner, J. Sullivan, *On the minimum ropelength of knots and links*, Invent. Math. **150** (2) pp 257-286 (2003)

[**FT**], D. Fuchs, S. Tabachnikov, *Mathematical Omnibus: Thirty Lectures on Classic Mathematics*, AMS 2007

[**HF**, D.F. Hinz, E. Fried, *Translation of Michael Sadowsky's paper 'An elementary proof for the existence of a developable MÖBIUS band and the attribution of the geometric problem to a variational problem'*. J. Elast. 119, 3–6 (2015)

[**HW**], B. Halpern and C. Weaver, *Inverting a cylinder through isometric immersions and embeddings*, Trans. Am. Math. Soc **230**, pp 41.70 (1977)

[**MK**] L. Mahadevan and J. B. Keller, *The shape of a Mobius band*, Proceedings of the Royal Society A (1993)

[**Sab** I.Kh. Sabitov, *Isometric immersions and embeddings of a flat Möbius strip in Euclidean spaces*, Izv. RAN. Ser. Mat. vol 71, issue 5, pp 197-224 (2007).

[**Sad**], M. Sadowski, *Ein elementarer Beweis für die Existenz eines abwickelbaren Möbiusschen Bandes und die Zurückführung des geometrischen Problems auf einVariationsproblem.* Sitzungsberichte der Preussischen Akad. der Wissenschaften, physikalisch-mathematische Klasse 22, 412–415.2 (1930)

[**SU**], M. Satoko, M. Umehara, *Flat Surfaces with Singularities in Euclidean 3-Space*, J. Diff Geo., 82(2), pp 279-316 (2009)

[**S1**] G. Schwarz, *A pretender to the title "canonical Moebius strip"*, Pacific J. of Math., **143** (1) pp. 195-200, (1990)

[**S2**] R. E. Schwartz, *The* 5 *Electron Case of Thomson's Problem*, Journal of Experimental Math, 2013.

[**W**] S. Wolfram, *The Mathematica Book, 4th Edition*, Wolfram Media and Cambridge University Press (1999).